Numerical Method for Nozzle Airflow Problem

Zamri Omar, Fatimah Yusop, Badrul Aisham Md Zain

Abstract—The divergent and convergent-divergent nozzles are discussed. The airflow problem inside the duct has a high degree of complexity, and is modeled by using Partial Differential Equation, which is then solved by using numerical approach. Finite Volume Method is used to solve the equation because its suitability for complex geometry problems. The study of airflow inside the nozzle is important in order to have a good nozzle configuration design that suits the intended applications.

Keywords—Nozzle airflow, numerical method, finite volume method, TVD scheme.

I. INTRODUCTION

NOZZLES are used in various applications such as jet engines, rocket propulsion, spray painting, and extrusion molding process. The use of nozzle is to control the rate of flow, velocity, direction, shape and pressure of the liquid that emerges from it. In supersonic nozzle design for example, the flow is compressible, and the approach of analysis is different with the incompressible flow model. The characteristic of the compressible flow in the nozzle is strongly depending on the physical design of the divergent-convergent section of the nozzle. In fact, the convergent-divergent shape of the nozzle is compulsory in order to achieve supersonic velocity [1,2,3]. In this paper we, discuss the use of numerical method to study the airflow inside the convergent-divergent nozzle.

Partial Differential Equation (PDE) function is widely used to model the fluid behavior mathematically. The airflow behavior can be examined quantitatively by solving the PDE through numerical approach. One of the numerical methods is Finite Volume Method (FVM), where it is a good solution for complex geometry [4]. The most common PDE that is used to model the airflow is hyperbolic equation which involved spatial derivatives and time marching. Hyperbolic equation has many schemes, the most common is the higher order Total Variation Diminishing (TVD) scheme.

Harteen [5] introduced the concept of TVD in order to overcome weak solution in hyperbolic conservation problem. The concepts used a non oscillatory first order accurate scheme to an appropriately modified the flux function [5,6].

Zamri Omar is a Senior Lecturer at Universiti Tun Hussein Onn Malaysia (UTHM), Parit 86400 Raja, Batu Pahat, Johor, Malaysia (phone: 607-4537618; fax: 607-4536080; e-mail: zamri@uthm.edu.my).

Fatimah Yusop is postgraduate student at Universiti Tun Hussein Onn Malaysia (UTHM), Parit 86400 Raja, Batu Pahat, Johor, Malaysia (e-mail: fatimahyusop@ymail.com).

Badrul Aisham Md Zain is a Senior Lecturer at Universiti Tun Hussein Onn Malaysia (UTHM), Parit 86400 Raja, Batu Pahat, Johor, Malaysia (e-mail: aisham@uthm.edu.my).

It is quite common to combine the TVD scheme with flux limiter. This flux limiter can control the amount of anti-diffusive flux. Therefore many types of flux limiter were introduced such as Harteen [5] and Roe Sweaby []. Additionaly, TVD scheme is not only limited to FDM, but it has been successfully applied in FVM. The result is quite good especially for complex unsteady airflow and strong shock problem [8].

The combination of TVD and Runge Kutta was initiated two decades ago where Runge-Kutta was used as multistage stepping time discretizations [9]. This scheme is widely used for stabilizing the spatial discretizations [10,11]. However, TVD Runge-Kutta scheme is only suitable for third-order and fourth-order equations. For the higher orders, this scheme becomes more complicated and less stability [11]. Another attempt to improve the TVD-Runge Kutta scheme was to modify the coefficient of each stage [12].

In developing the computational fluid dynamics (CFD) code, the most convenient way is to start with a less complicated one-dimensional (1-D) airflow problem, followed by higher fidelity of two or three-dimensional models. Through the solution of 1-D airflow problem, it is relatively quick and easy to identify the effectiveness of the CFD code and also to detect errors due to coding and the numerical scheme limitation itself.

The development of the computer code for solving two or three dimensional airflow problems uses TVD Runge-Kutta scheme with FVM approach for its spatial discretization. The space inside the duct is modeled as a nozzle, where the quasi one dimensional airflow passes through it. Two different types of nozzles are investigated which are divergent and convergent-divergent. The airflow conditions inside the nozzle may be fully isentropic airflow over the whole nozzle or with shock wave may exist at some points in the divergent part of the nozzle.

II. GOVERNING EQUATION

The airflow pass through a nozzle can be considered as the airflow pass through a slow varying cross section. As a result, the airflow problem can be considered as a quasi one dimensional airflow. In addition, the viscous effect can be ignored, so the Euler equation may represent the most appropriate equation to describe the airflow behavior throughout the nozzle.

The Euler equation can be presented in various forms such as conservative, non conservative, scalar or vector notation forms. When the presence of the shock wave in the airflow

field is considered as a part of the solution, the appropriate form of the governing equation of fluid motion is in the conservative and vector notation. The Euler Equation in this form can be written as [13,14]:

$$\frac{\partial W}{\partial t} + \frac{\partial F}{\partial x} - Q = 0 \tag{1}$$

$$W = \begin{bmatrix} \rho A \\ \rho u A \\ \rho E A \end{bmatrix}, F = \begin{bmatrix} \rho u A \\ (\rho u^2 + p)A \\ \rho H u A \end{bmatrix}, Q = \begin{bmatrix} 0 \\ p \, dA/dx \\ 0 \end{bmatrix} \tag{2a, 2b, 2c}$$

Here W, F and Q denote the conservative variable, flux vectors and source term respectively. Meanwhile, ρ, u, p, E, H and A are density, velocity, pressure, total energy, enthalpy and cross section area respectively. For the perfect gas, there is a unique relation between pressure p, H and internal energy, e given as:

$$E = e + \frac{u^2}{2}, H = E + \frac{p}{\rho}, p = (\gamma - 1)\rho\left(E - \frac{u^2}{2}\right) \tag{3a, 3b, 3c}$$

The space discretization is done based on the following two schemes:

A. Second Order TVD Scheme

Based on (1), TVD formulation can be derived as [11],

$$W_i^{n+1} = W_i^n - \frac{1}{A}\left(\frac{\Delta t}{\Delta x}\right)\left[R_{i+1/2}^n - R_{i-1/2}^n\right] + \frac{\Delta t}{A}Q_i^n \tag{4}$$

where,

$$R_{i+1/2}^n = \frac{1}{2}\left(E_{i+1}^n + E_i^n + X_{i+1/2}^n \Phi_{i+1/2}^n\right) \tag{5a}$$

and,

$$R_{i-1/2}^n = \frac{1}{2}\left(E_i^n + E_{i-1}^n + X_{i-1/2}^n \Phi_{i-1/2}^n\right) \tag{5b}$$

where X is eigenvector in matrix form and Φ is the flux limiter. In this paper, three limiter models are used, which are Harteen-Yee Upwind TVD, Roe-Sweaby Upwind TVD and Davis-Yee Symmetric TVD. The Harteen-Yee Upwind TVD can be written as follows;

$$\phi_{i-1/2} = \sigma(\alpha_{i-1/2})(G_i + G_{i-1}) - \psi(\alpha_{i-1/2} + \beta_{i-1/2}) \, \delta_{i-1/2} \tag{6a}$$

$$\phi_{i-1/2} = \sigma(\alpha_{i-1/2})(G_i + G_{i-1}) - \psi(\alpha_{i-1/2} + \beta_{i-1/2}) \delta_{i-1/2} \tag{6b}$$

with limiter defined as,

$$G_i = \min \operatorname{mod}(\delta_{i-1/2}, \delta_{i+1/2}) \tag{7a}$$

$$G_i = \frac{\delta_{i+1/2}\delta_{i-1/2} + |\delta_{i+1/2}\delta_{i-1/2}|}{\delta_{i+1/2} + \delta_{i-1/2}} \tag{7b}$$

$$G_i = \frac{\delta_{i-1/2}\left[(\delta_{i+1/2})^2 + \omega\right] + \delta_{i+1/2}\left[(\delta_{i-1/2})^2 + \omega\right]}{(\delta_{i+1/2})^2 + (\delta_{i-1/2})^2 + 2\omega} \tag{7c}$$

where $10^{-7} \le \omega \le 10^{-5}$. The Roe-Sweaby Upwind TVD can be written as follows;

$$\phi_{i+1/2} = \left[\frac{G_i}{2}\left(|\alpha_{i+1/2}| + \frac{\Delta t}{\Delta x}\alpha_{i+1/2}^2\right) - |\alpha_{i+1/2}|\right]\delta_{i+1/2} \tag{8a}$$

$$\phi_{i+1/2} = \left[\frac{G_i}{2}\left(|\alpha_{i+1/2}| + \frac{\Delta t}{\Delta x}\alpha_{i+1/2}^2\right) - |\alpha_{i+1/2}|\right]\delta_{i+1/2} \tag{8b}$$

with limiter defined as,

$$G_i = \min \operatorname{mod}(1, r) \tag{9a}$$

$$G_i = \frac{r + |r|}{1 + r} \tag{9b}$$

$$G_i = \max[0, \min(2r, 1), \min(r, 2)] \tag{9c}$$

where,

$$r = \begin{cases} \dfrac{X_{i+1+\sigma}^{-1}Q_{i+1+\sigma} - X_{i+\sigma}^{-1}Q_{i+\sigma}}{\delta_{i+1/2}} & \text{for} \quad \delta_{i+1/2} \ne 0 \\ 0 & \text{for} \quad \delta_{i+1/2} = 0 \end{cases} \tag{10}$$

The Davis-Yee Symmetric Upwind TVD can be written as follows;

$$\phi_{i+1/2} = -\left[\frac{\Delta t}{\Delta x}(\alpha_{i+1/2})^2 G_{i+1/2} + \psi(\alpha_{i+1/2} - G_{i+1/2})\right] \tag{11}$$

with limiter defined as,

$$G_{i+1/2} = \min \operatorname{mod}\left[2\delta_{i-1/2}, 2\delta_{i+1/2}, 2\delta_{i+3/2}, \frac{1}{2}(\delta_{i-1/2} + \delta_{i+3/2})\right] \tag{12a}$$

$$G_{i+1/2} = \min \operatorname{mod}[\delta_{i-1/2}, \delta_{i+1/2}, \delta_{i+3/2}] \tag{12b}$$

$$G_{i+1/2} = \min \operatorname{mod}[\delta_{i+1/2}, \delta_{i-1/2}] + \min \operatorname{mod}[\delta_{i+1/2}, \delta_{i+3/2}] - \delta_{i+1/2} \tag{12c}$$

B. Central And Multistage Scheme

Time integration in executed by using explicit multistage time-marching (Runge-Kutta scheme), while central difference scheme with artificial dissipation is used for spatial discretization. The artificial dissipation can be written as [12]:

$$D_{i+1/2} = (\hat{\Lambda}_c^I)_{i+1/2}\left[\varepsilon_{i+1/2}^{(2)}(W_{i+1} - W_i) - \varepsilon_{i+1/2}^{(4)}(W_{i+2} - 3W_{i+1} + 3W_i - W_{i-1})\right] \tag{13}$$

The spectral radius at the cell faces as follows;

$$(\hat{\Lambda}_c^I)_{i+1/2} = \frac{1}{2}\left[(\hat{\Lambda}_c^I)_i + (\hat{\Lambda}_c^I)_{i+1}\right] \tag{14a}$$

$$\hat{\Lambda}_c = (|V| + c)\Delta A \tag{14b}$$

where V is the velocity and c is the speed of sound. Thus, the total convective flux at face (i+1/2) can written as,

$$(F_c \Delta A)_{i+1/2} \approx F_c(W_{i+1/2}) \Delta A_{i+1/2} - D_{i+1/2} \qquad (15)$$

where W is the average airflow variable. Multistage time stepping is the solution in a number of steps, where it will give updates on the airflow variable in each stage, from the first to the last (m-stage) as follows:

$$W_i^{(0)} = W_i^n$$

$$W_i^{(1)} = W_i^{(0)} - \alpha_1 \frac{\Delta t}{V} R_i^{(0)}$$

$$W_i^{(2)} = W_i^{(0)} - \alpha_2 \frac{\Delta t}{V} R_i^{(1)} \qquad (16)$$

$$\vdots$$

$$W_i^{n+1} = W_i^m = W_i^{(0)} - \alpha_m \frac{\Delta t}{V} R_i^{m-1}$$

III. DIVERGENT NOZZLE

For divergent nozzle, the investigation deals with two airflow problems which are a purely supersonic isentropic airflow and a supersonic-subsonic airflow with a normal shock standing inside the nozzle. The distribution of the cross section along the nozzle in given in Fig. 1, derived from Eq. (17) which is found in [11].

$$A(x) = 1.398 + 0.347 \tanh(0.8 - 4) \qquad (17)$$
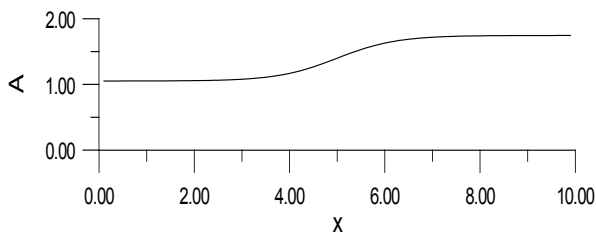
Fig. 1: Divergent nozzle cross section

IV. CONVERGENT-DIVERGENT NOZZLE

For convergent divergent nozzle, the airflow is initially subsonic at the convergent part. By assuming the airflow condition is reaching the chocked condition, it makes the airflow in the remaining airflow domain may go to supersonic until at the exit nozzle station or end up with subsonic speed due to shock wave occurred somewhere inside the divergent part.

$$A(x) = 1 + \frac{1}{2}(A_1 - 1)\left\{1 + \cos\left(\frac{\pi x}{x_{thr}}\right)\right\} \qquad \text{for} \quad 0 \le x \le x_{thr} \qquad (18)$$

$$A(x) = 1 + \frac{1}{2}(A_2 - 1)\left\{1 - \cos\left[\frac{\pi(x - x_{thr})}{1 - x_{thr}}\right]\right\} \qquad \text{for} \quad x_{thr} \le x \le 1$$

Fig.2 shows the graphical representation of the cross sectional area varations throughout the divergent nozzle, which is modeled by using Eq. (18) found in [12].
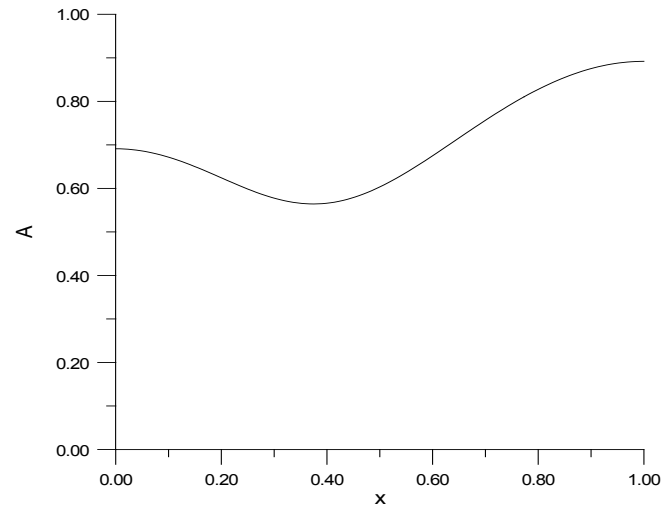

Fig. 2: Convergent-Divergent nozzle cross section

V. RESULT ANF DISCUSSION

For divergent nozzle, the setting of airflow condition is given as follows:

a. At entry (inflow) station :
   i. Mach number, $M = 1.75$
   ii. Pressure, $p = 1800.0$ Ib/ft^2
   iii. Temperature, $T = 500.0$ °R

b. At exit (outflow) station:
   i. Supersonic outflow – no data required
   ii. Subsonic outflow – Velocity, $v = 566.433$

For convergent-divergent nozzle, the setting of the airflow condition is given as follows:

c. At entry (inflow) station :
   i. Total Pressure, $P_0 = 1.0 \times 10^5$ Pa
   ii. Total Temperature, $T_0 = 288.0$ K

d. At exit (outflow) station:
   i. Supersonic outflow – no data required
   ii. Subsonic outflow – Pressure, $p = 0.7 \times 10^5$ Pa

By using these airflow conditions, the calculation was carried out by three different numerical schemes, with each scheme uses three limiter models. The Harten-Yee TVD scheme combined with the flux limiter function as defined by Eq.7a, Eq. 7b and Eq. 7c. For the Roe-Sweby TVD scheme,

the flux limiter function is implanted in the developed computer code as given in Eq. 9a, Eq. 9b and Eq. 9c. The Davis-Yee TVD scheme with the limiter models as stated in Eq. 12a, Eq. 12b and Eq. 12c.

The Mach number and pressure distributions along the divergent nozzle for Davis Yee TVD scheme with three different flux limiter functions are shown in Fig. 3a and Fig. 3b respectively. From both plots, it is very clear that all three different flux limiters give nearly similar results. In Fig. 3a, we notice that the Mach number grows exponentially, started at the beginning of the divergent section of the nozzle. The Mach number reached 2.4 and it remains constant throughout the nozzle.

This Mach number trend is following the theoretical of supersonic flow inside the divergent nozzle. In fact, it is compulsory to have divergent nozzle in order to reach the supersonic flow. The corresponding airflow pressure is given in Fig. 3b where it shows the reduction of pressure in the manner that is opposite of the Mach number.
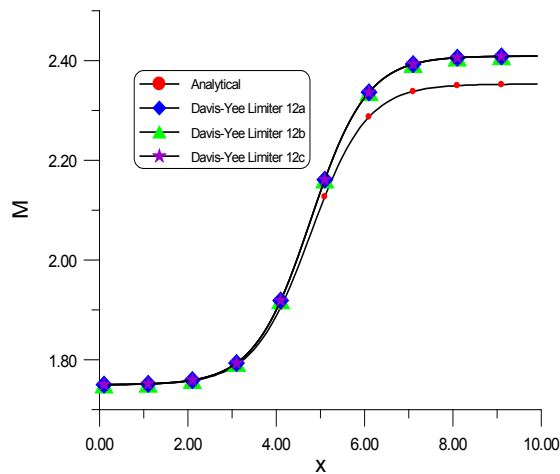
Fig. 3a: Comparison of Mach number distribution of isentropic airflow by TVD Runge Kutta scheme with Davis-Yee limiter for Nozzle A inflow.
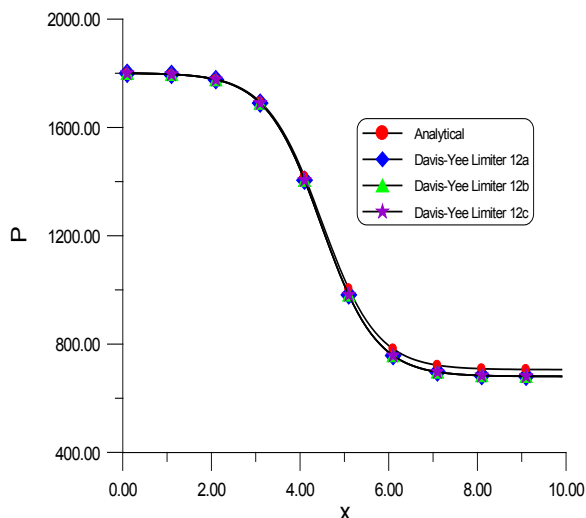
Fig. 3b: Comparison of pressure distribution of isentropic airflow by TVD Runge Kutta scheme with Davis-Yee limiter

for Nozzle A inflow.

In the upstream side, it is very clear that the Davis-Yee TVD schemes are able to provide solutions which are very close to the solution obtained through the analytical method. However, a quite noticeable difference appeared at far down stream airflow section where the Mach number and pressure distribution obtained through analytical solution are smaller compared to the numerical solution. Similar trend of the result is also found for Harten-Yee and Roe-Sweby TVD schemes. This can be seen in Fig. 4 and Fig. 5.
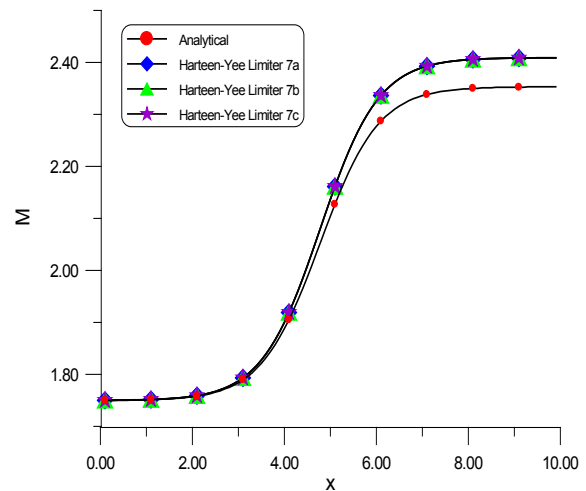

Fig. 4a: Comparison of Mach number distribution of isentropic airflow by TVD Runge Kutta scheme with Harteen-Yee limiter for Nozzle A inflow.
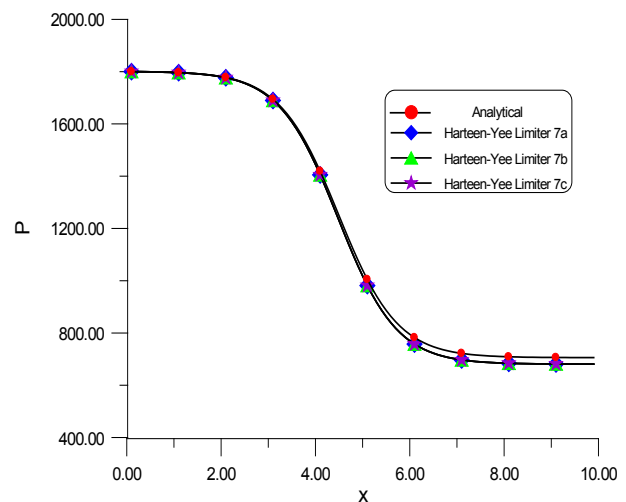

Fig. 4b: Comparison of pressure distribution of isentropic airflow by TVD Runge Kutta scheme with Harteen-Yee limiter for Nozzle A inflow.
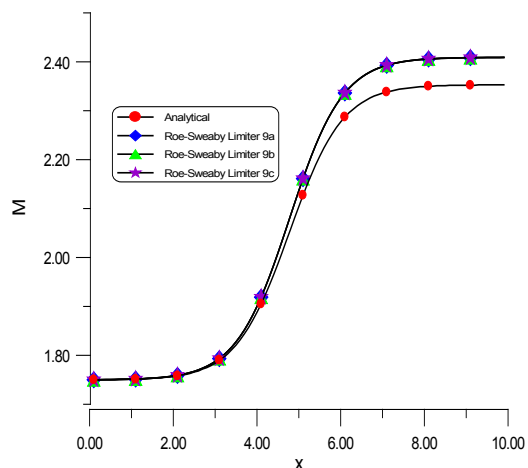
Fig. 5a: Comparison of Mach number distribution of isentropic airflow by TVD Runge Kutta scheme with Roe-Sweaby limiter for Nozzle A inflow.
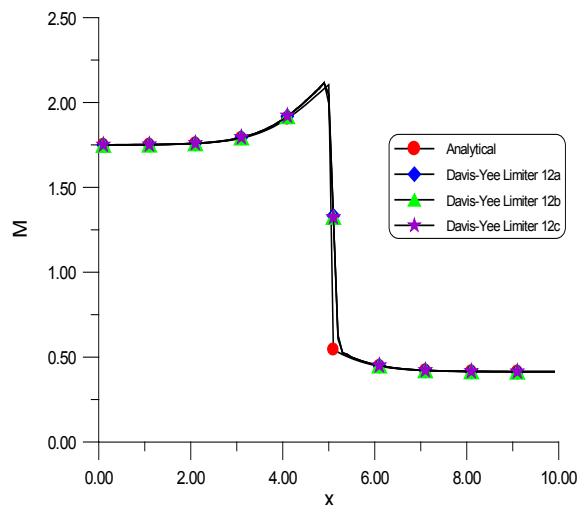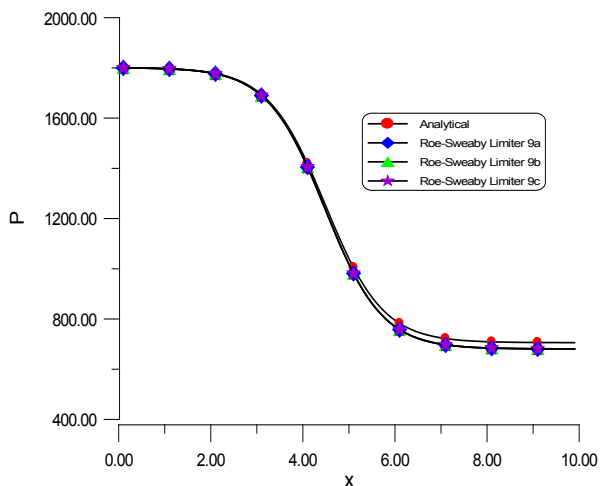

Fig. 5b: Comparison of pressure distribution of isentropic airflow by TVD Runge Kutta scheme with Roe-Sweaby limiter for Nozzle A inflow.
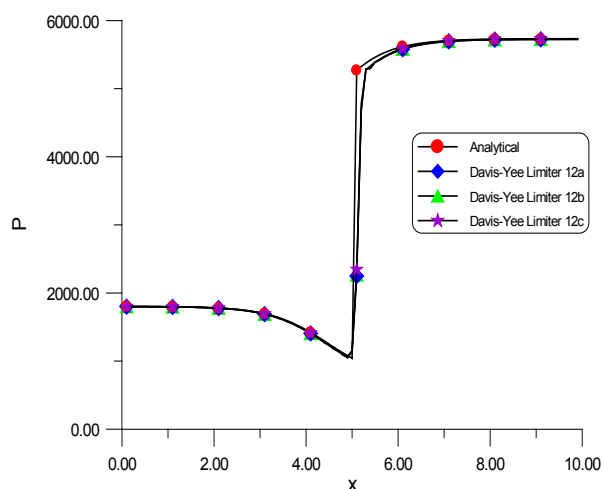
Meanwhile, Fig. 6, Fig. 7 and Fig. 8 show the results for subsonic outflow of the divergent nozzle. These plots indicate that the shock wave occurred at the middle section of divergent nozzle. The prediction of shock position as seen in these plots is well agreed with the analytical prediction. This indicated that shock wave occurred at approximately at 50% of the duct length.

Also depicted in Fig. 7 and Fig. 8, the predictions of the flow are quite similar although different flux limiters were applied on the schemes. These trends are also similar with the analytical predictions. This proves that the numerical approach is quite good for shock wave problem.
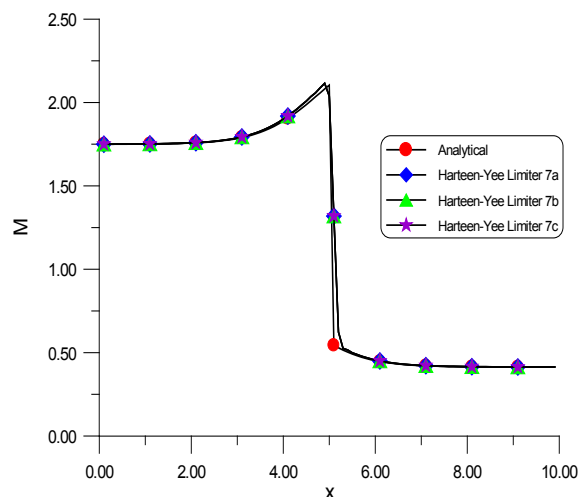

Fig. 6a: Comparison of Mach number distribution of shock problem by TVD Runge Kutta scheme with Davis-Yee limiter for outflow Nozzle A outflow.

Fig. 6b: Comparison of pressure distribution of shock problem by TVD Runge Kutta scheme with Davis-Yee limiter for Nozzle A outflow.

Fig. 7a: Comparison of Mach distribution of shock problem by TVD Runge Kutta scheme with Harteen-Yee limiter for
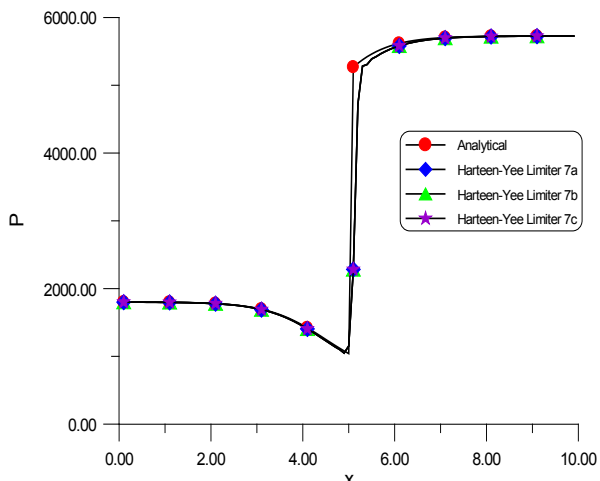
Nozzle A outflow.

Fig. 7b: Comparison of pressure distribution of shock problem by TVD Runge Kutta scheme with Harteen-Yee limiter for Nozzle A outflow.
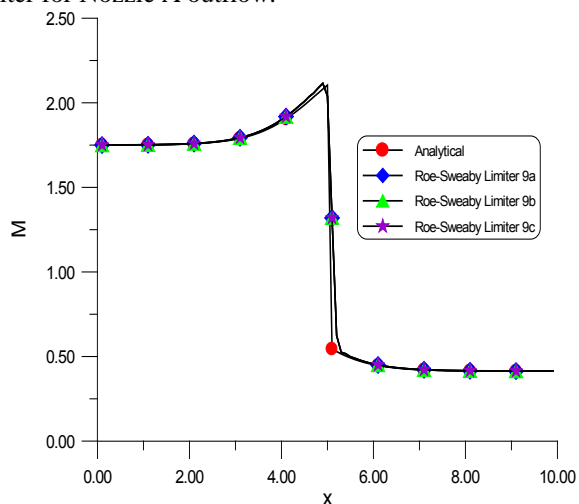

Fig. 8a: Comparison of Mach number distribution of shock problem by TVD Runge Kutta scheme with Roe-Sweaby limiter for Nozzle A outflow.
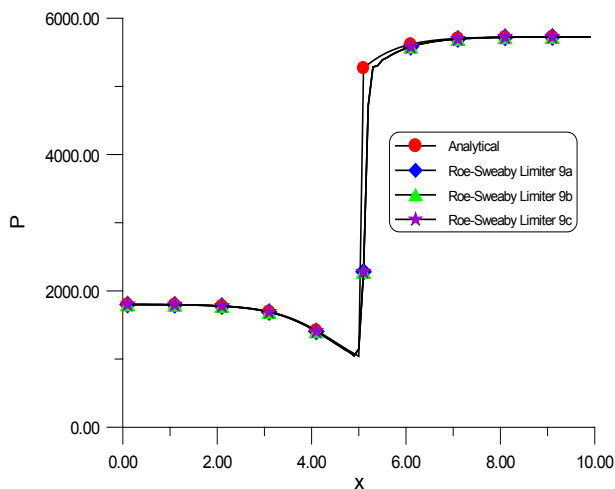

Fig. 8b: Comparison of Mach number distribution of shock

problem by TVD Runge Kutta scheme with Roe-Sweaby limiter for Nozzle A outflow.

Fig. 9, Fig. 10 and Fig. 11 show the result for flow predictions in Nozzle B. The flow is subsonic at both inflow and outflow. However, the occurrence of shock wave causes the airflow becomes supersonic at the middle of the nozzle. Both approaches show that the shock wave occurred at the location after the throat, at approximately 64% of the nozzle length. The comparison with analytical shows that the flux limiters given nearly similar results.
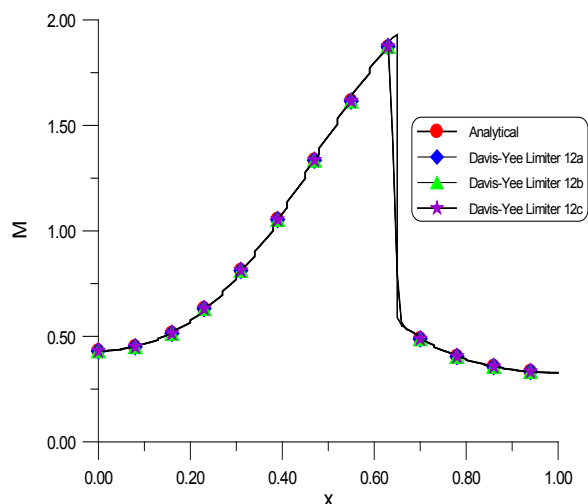

Fig. 9a: Comparison of Mach number distribution of shock problem by TVD Runge Kutta scheme with Davis-Yee limiter for Nozzle B inflow.
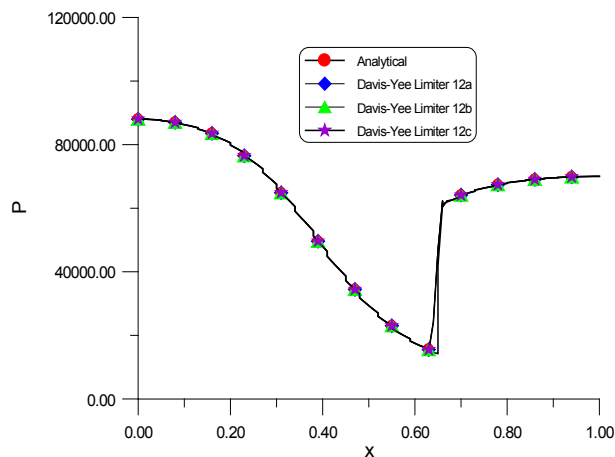

Fig. 9b: Comparison of pressure distribution of shock problem by TVD Runge Kutta scheme with Davis-Yee limiter for Nozzle B inflow.
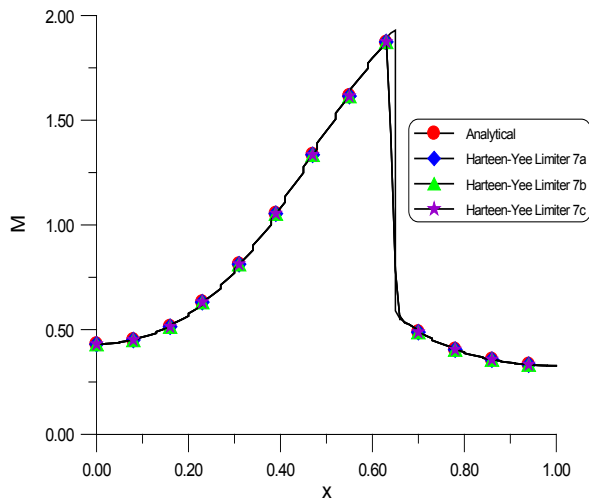
Fig. 10a: Comparison of Mach distribution of shock problem by TVD Runge Kutta scheme with Davis-Yee limiter for Nozzle B inflow.
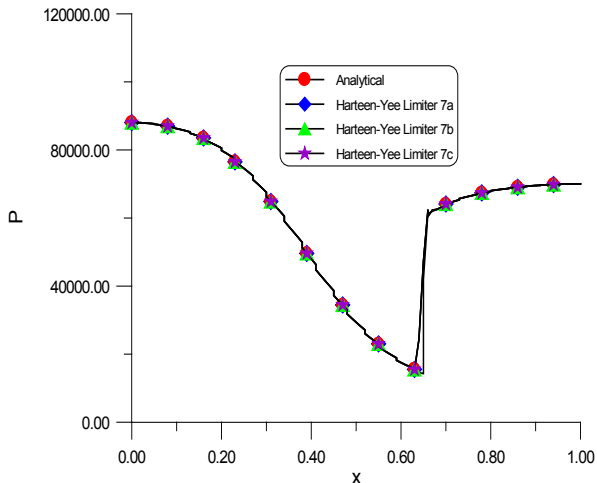

Fig. 10b: Comparison of pressure distribution of shock problem by TVD Runge Kutta scheme with Davis-Yee limiter for Nozzle B inflow.
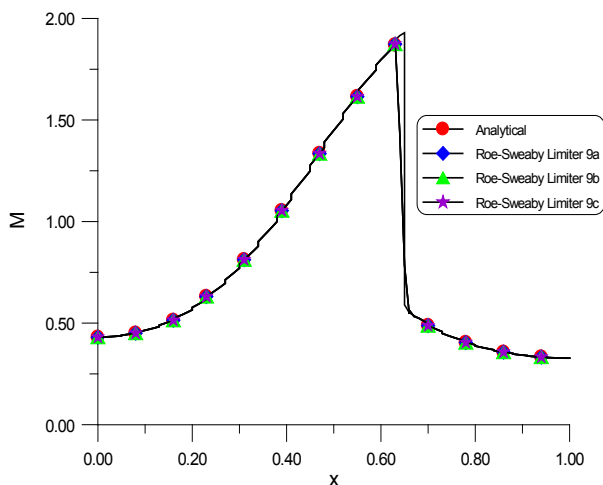

Fig. 11a: Comparison of Mach number distribution of shock problem by TVD Runge Kutta scheme with Roe-Sweaby limiter for Nozzle B outflow.

VI. CONCLUSION

In this paper, the chosen numerical approach, FVM TVD Runge-Kutta was successfully implemented for 1-D nozzle cases. These include the isentropic airflow, shock wave problem for two types of nozzle geometry. The comparison with the analytical solution gives a good agreement for all types of limiters. In addition, the used of three different limiters were result in similar airflow predictions.

Varying the flux limiters affects the pressure and Mach number in the nozzle, but it is not significant. The applied numerical approach is also performed very well in predicting the shock wave of the airflow. This numerical approach is an appropriate numerical scheme to solve 1-D airflow problem inside the duct. The study should be extended to solve the two and three dimensional airflow problem of the nozzle. A thorough observation of the airflow pattern inside the nozzle is very important in preparing the suitable nozzle design for various applications.

REFERENCES

[1]. John D. Anderson. *Fundamental of Aerodynamics*, McGraw Hill, New York, 2012.

[2]. John J. Bertin. *Aerodynamics For Engineers*, Prentice Hall, 2013.

[3]. Gary M. Ullrich, Mark J. Dusenbury. *Aerodynamics*, Kendall Hunt Publishing, 2012.

[4]. Chung, T.J. *Computational Fluid Dynamics*. 2nd Ed. New York: Cambridge University Press, 2002.

[5]. Harten, A.. *High resolution schemes for hyperbolic conservation laws*. Journal of Computational Physics. 49, 357-393, 1983.

[6]. Chang, S. H. *A numerical study of ENO and TVD schemes for shock capturing*. NASA Technical Memorandum 101355, 1988.

[7]. Sweby, P. K. .*High resolution using flux limiters for hyperbolic conservation laws*. SIAM J. Science and Statistics Computation, 21(5), 995-1011, 1983.

[8]. Choi, H. S. & Baek, J. H. *Computations of nonlinear wave interaction in shock-wave focusing process using finite volume TVD schemes. Computers & Fluids. 25(5), 509-522,* 1996.

[9]. Shu, C. W. *Total-variation-diminishing time discretizations. SIAM J. Sci. and Stat. Comput., 9(6), 1073-1084,* 1988.

[10]. Gottlieb, S. & Shu, C. W. *Total variation diminishing Runge-Kutta schmes. Mathematics of Computation*. 67, 73-85, 1988.

[11]. Bagabir, A. & Drikakis, D. *Numerical experiments using high-resolution schemes for unsteady, inviscid, compressible airflows*. Computational. Methods Appllication Mech. Engineering, 193 4675-4705. 2004.

[12].Park, T. S. & Kwon, J. H. *An improved multistage time stepping for second-order upwind TVD schme. Computers & Fluids. 25(7), 629-645*, 1996.

[13].Hoffmann, K.A. & Chiang, S.T. *Computational Fluid Dynamics Volume II*. 4th ed. USA, 2002.

[14].Blazek, J. *Computational Fluid Dynamics: Principles and Applications*. Elsivier, 2005.